International Journal of Obesity
https://doi.org/10.1038/s41366-019-0367-3

ARTICLE

Adipocyte and Cell Biology

GALNT2 as a novel modulator of adipogenesis and adipocyte insulin signaling

Antonella Marucci[1] · Alessandra Antonucci[1,2] · Concetta De Bonis[1] · Davide Mangiacotti[1] · Maria Giovanna Scarale[1] · Vincenzo Trischitta[1,3] · Rosa Di Paola[1]

Received: 12 September 2018 / Revised: 25 February 2019 / Accepted: 15 March 2019

Abstract

Background/objectives A better understanding of adipose tissue biology is crucial to tackle insulin resistance and eventually coronary heart disease and diabetes, leading causes of morbidity and mortality worldwide. GALNT2, a GalNAc-transferase, positively modulates insulin signaling in human liver cells by down-regulating ENPP1, an insulin signaling inhibitor. GALNT2 expression is increased in adipose tissue of obese as compared to that of non-obese individuals. Whether this association is secondary to a GALNT2-insulin sensitizing effect exerted also in adipocytes is unknown. We then investigated in mouse 3T3-L1 adipocytes the GALNT2 effect on adipogenesis, insulin signaling and expression levels of both *Enpp1* and 72 adipogenesis-related genes.

Methods Stable over-expressing GALNT2 and GFP preadipocytes (T_0) were generated. Adipogenesis was induced with ($R+$) or without ($R-$) rosiglitazone and investigated after 15 days (T_{15}). Lipid accumulation (by Oil Red-O staining) and intracellular triglycerides (by fluorimetric assay) were measured. Lipid droplets (LD) measures were analyzed at confocal microscope. Gene expression was assessed by RT-PCR and insulin-induced insulin receptor (IR), IRS1, JNK and AKT phosphorylation by Western blot.

Results Lipid accumulation, triglycerides and LD measures progressively increased from T_0 to $T_{15}R-$ and furthermore to $T_{15}R+$. Such increases were significantly higher in GALNT2 than in GFP cells so that, as compared to $T_{15}R+$GFP, $T_{15}R-$ GALNT2 cells showed similar (intracellular lipid and triglycerides accumulation) or even higher (LD measures, $p < 0.01$) values. In GALNT2 preadipocytes, insulin-induced IR, IRS1 and AKT activation was higher than that in GFP cells. GALNT2 effect was totally abolished during adipocyte maturation and completely reversed at late stage maturation. Such GALNT2 effect trajectory was paralleled by coordinated changes in the expression of *Enpp1* and adipocyte-maturation key genes.

Conclusions GALNT2 is a novel modulator of adipogenesis and related cellular phenotypes, thus becoming a potential target for tackling the obesity epidemics and its devastating sequelae.

Introduction

Obesity and adipose tissue dysfunction are major movers of insulin resistance, thus predisposing to leading causes of morbidity and mortality [1], such as coronary heart disease and type 2 diabetes [2]. A better understanding of the mechanisms controlling adipogenesis is therefore of crucial importance.

These authors contributed equally: Antonella Marucci, Alessandra Antonucci

Supplementary information The online version of this article (https://doi.org/10.1038/s41366-019-0367-3) contains supplementary material, which is available to authorized users.

✉ Vincenzo Trischitta
vincenzo.trischitta@operapadrepio.it

✉ Rosa Di Paola
r.dipaola@operapadrepio.it

[1] Research Unit of Diabetes and Endocrine Diseases, Fondazione IRCCS "Casa Sollievo della Sofferenza", San Giovanni Rotondo, Italy

[2] Department of Molecular Medicine, Sapienza University, Rome, Italy

[3] Department of Experimental Medicine, Sapienza University, Rome, Italy

Published online: 30 April 2019

Insulin stimulates lipid storage in adipocytes [3]. So, it is not surprising that insulin sensitivity prospectively predicts weight gain increase [4]. Further confirming that insulin sensitivity positively controls body weight is the common observation that thiazolidinediones—insulin sensitizing molecules used as anti-hyperglycemic drugs in type 2 diabetes—increase body mass index (BMI) [5].

GALNT2, a GalNAc-transferase [6] involved in O-linked glycosylation [7], modulates the risk of atherogenic dyslipidemia [8–11], a specific hallmark of insulin resistance and acts as a positive modulator of insulin signaling in human liver cells, by down-regulating ENPP1, an inhibitor of insulin receptor (IR) [12]. Interestingly, GALNT2 expression in subcutaneous adipose tissue is increased in obese, insulin resistant individuals as compared to their non-obese counterparts [13]. Whether this association underlies a cause-effect relationship, with GALNT2 firstly predisposing to weight gain by exerting a positive modulation on adipose tissue insulin signaling and eventually concurring to develop obesity and the inevitably related insulin resistance, is a reasonable possibility that has never been addressed. In order to get deeper insights about this hypothesis, we investigated in cultured mouse adipocytes the effect of GALNT2 on adipogenesis, lipid accumulation and insulin signaling.

Materials and methods

Cell culture

Both mycoplasma-free 3T3-L1 murine fibroblast (Addex-Bio), and 293T cells (ATCC) were routinely cultured in high-glucose Dulbecco's modified Eagle's medium (DMEM) (Sigma-Aldrich) supplemented with 10% fetal bovine serum (FBS) (EuroClone) and maintained at 37 °C in a humidified atmosphere with 5% CO_2.

Recombinant Lentivirus production and transduction

Human ORF *GALNT2* cloned into pLX304 vector under CMV promoter (pLXGALNT2) and both dR8.91 (Packaging plasmid) and VSV-G (Envelope plasmid), used for lentiviral production, were purchased from Harvard Medical School Facilities. Plasmid pRRL-PGK-GFP was kindly provided by F. Carlotti (Nice, FR) [14].

Lentiviral particles were generated by co-transfecting either pLXGALNT2 or pRRL-PGK-GFP with both dR8.91 and VSV-G plasmids in 293T cells by calcium phosphate method [15]. Cells were then maintained in DMEM supplemented with 30% FBS for 18 h and lentiviral particles harvested, filtered through 0.45 µm filter and stored at −80 °C until used.

In order to obtain 3T3-L1 cell lines over-expressing either GFP (GFP cells) or GALNT2 (GALNT2 cells), both viral supernatants were added to fresh medium supplemented with 8 µg/ml Polybrene (Sigma-Aldrich) and 3T3-L1 cells incubated overnight. After 24 h, the medium was replaced with fresh DMEM plus 10% FBS and, then, changed every 2 days. GALNT2 transduced cells were further selected by adding 5 µg/ml of blasticidin (Thermo Fisher Scientific). GFP cells were used as control in all experiments.

3T3-L1 adipocytes differentiation

Cells were seeded either in 6-well-plates (Sigma-Aldrich) or in 18 × 18 mm sterile imaging glasses, at ~8×10^3cell/cm^2 cell density and grown in DMEM plus 10% FBS for 4 days in order to obtain 100% confluence (T_0 GFP and T_0 GALNT2 cells). Cell differentiation was induced, by using DMEM plus 1 µM dexamethasone (Calbiochem), 0.5 mM 1-methyl-3-isobutylxanthine (Calbiochem), 5 µg/ml human recombinant insulin (Gibco) and either with (*R*+) or without (*R*−) 2 µM rosiglitazone (Cayman Chemical). After 48 h, *R*+ and *R*− differentiation mediums were replaced with 10% FBS supplemented DMEM plus either 5 µg/ml insulin, with a biweekly medium replacement until day 15 (T_{15} GFP and T_{15} GALNT2 cells).

Oil Red O staining and lipid quantification

Oil Red-O (ORO) staining was performed in T_0, $T_{15}R-$ and $T_{15}R+$cells as it follows. Briefly, cells were fixed with 10% formalin for at least 1 h, rinsed with 60% isopropyl alcohol and, after complete drying, treated with ORO for 10 min. Cells were then washed 4 times with deionized H_2O and dried. Embedded ORO, an inferred measures of intracellular lipids, was eluted, by adding 100% isopropyl alcohol for 10 min, and quantified at 500 nm by Synergy-HT spectrophotometer (Bio-Tek). The resulting optical densities (OD) were expressed as percentage on either T_0 GFP or T_0 GALNT2 cells, respectively.

Intracellular triglycerides levels were measured in T_0, $T_{15}R-$ and $T_{15}R+$cells by means of the fluorimetric enzymatic Adipogenesis Assay Kit according to manufacturer's instruction (Sigma-Aldrich). The resulting fluorimetric intensities were measured at 587 nm by Synergy-HT Fluorimeter (Bio-Tek), plotted versus a triglycerides standard curve and expressed as nmol/5000 cells.

Adipo Red staining

T_0, $T_{15}R-$ and $T_{15}R+$cells were rinsed twice with phosphate-buffer saline (PBS), fixed with 4% paraformaldehyde for 15 min and then incubated with Adipo Red

stain (Lonza) for 10 min. Next, cells were washed with PBS and adipocyte lipid droplets (LD) imaged.

Imaging

ORO-stained cells were imaged in bright field by means of an inverted microscope (Axiovert 2 M, Zeiss) at ×5 magnification (Zeiss FLUAR 5 × /0.25na objective).

Images' acquisition of Adipo Red-stained adipocytes was performed by using a TCS SP8 confocal microscope (Leica) at ×40 magnification (HC PL APO CS2 40 × /1.30 OIL Leica objective). At least 30 independent micrographs were acquired for each experimental condition. LD morphology was then analyzed by using Cell Profiler software. Briefly, images were segmented to identify lipids as discrete "objects" and then area and Feret's diameter (which account for LD size, in terms of diameter for rounded objects or major axis for irregular objects) were measured.

Western blot analysis

Cell lysates were separated by SDS-PAGE and transferred to nitrocellulose membrane Trans-Blot Turbo Transfer pack (Biorad). Blots were probed with specific antibodies, including anti-GALNT2 (ab97741, Abcam), anti β-Actin (sc-47778, Santa Cruz Biotechnology), anti-IR β-subunit (sc-711, Santa Cruz Biotechnology), anti-Phospho-IRS1^{Tyr895} (3070, Cell Signaling), anti-IRS1 (2382, Cell Signaling), anti-phospho-JNK1/JNK2$^{Thr183/Tyr185}$ (700031 Thermo Fisher Scientific), anti-JNK (9252, Cell Signaling), anti-Phospho-AKT^{Ser473} (9271, Cell Signaling) and anti-AKT (9272, Cell Signaling). Immune-complexes were then detected with the Super-Signal^{TM} West Pico (Thermo Fisher Scientific). Gel images were acquired by using Molecular Imager ChemiDoc XRS (Biorad) and band intensities quantified by Kodak Molecular Imaging Software 4.0 as OD values.

Insulin signaling

Cells were starved for 18 h with DMEM plus 0.5% FBS, stimulated with 10^{-7} M insulin for 5 min at 37 °C, and then washed with PBS and lysed. To evaluate IR β-subunit autophosphorylation, 300 µg of total lysate were immunoprecipitated with anti-PY99 antibody (sc-7020, Santa Cruz Biotechnology) and analyzed by Western blot as described above. To evaluate IRS1, JNK and AKT activation, 50 µg of total lysate were subjected to SDS-Page and IRS1^{Tyr895}, JNK1/JNK2$^{Thr183/Tyr185}$ and AKT^{Ser473} phosphorylation evaluated by western blot (see above). IRS1^{Tyr895}, JNK1/JNK2$^{Thr183/Tyr185}$ and AKT^{Ser473} phosphorylation levels were normalized against IRS1, JNK and AKT content. All data were calculated as percentage of insulin-stimulated GFP adipocytes and expressed as means ± SE.

RNA extraction, cDNA synthesis, and gene expression analysis

Total RNA was isolated from mature adipocytes by using RNeasy Mini kit (Qiagen). cDNA was generated by reverse transcription with iScript™ Reverse Transcription Supermix for RT-qPCR (Biorad) according to the manufacturer's instructions and used as template for subsequent analyses. Expression levels of 72 adipogenesis-related genes (Gene Target List can be found in Supplementary Information 1) were assessed by means of pre-designed Adipogenesis M384 SYBR green panels (Biorad), on ABI-PRISM 7900 (Applied Biosystems). Among 8 reference genes (see Supplementary Information 1), *β-actin*, *Gusb* and *Hsp90ab1* were chosen as those showing the best control gene-stability measured as indicated by M value (i.e., $M < 0.5$) across samples [16]. PrimeTime qPCR Probe Assays (Integrated DNA Technologies) were used to measure expression levels of *Ennp1* (Mm.PT.58.7142160), m*Galnt2* (Mm.PT.58.5475747) and *hGALNT2* (Hs.PT.58.3633908) on ABI-PRISM 7900 (Applied Biosystems). Gene expression levels were reported as ΔΔCq, calculated as relative gene quantity normalized to the geometric mean of reference genes (PrimePCR™ Analysis Software, Biorad).

Statistical analyses

Each experiment, for each condition, has been carried out at least 3 times in duplicate. Differences between mean values were evaluated by Student's *t*-test; a two sided p-values < 0.05 were considered for statistical significance. Data are presented as means ± SE. Analyses were performed by using SAS Software, Release 9.4 (SAS Institute, Cary, NC, USA).

Results

Over-expression of GALNT2 in 3T3-L1 cells

Firstly, 3T3-L1 cell lines expressing either GFP (GFP cells) or GALNT2 (GALNT2 cells) were created as described in methods. As compared to GFP cells, a clear band representing human GALNT2 was detectable at ~60 KDa in GALNT2 cells at both T_0 (preadipocytes, Fig. 1a) and T_{15} (mature adipocytes, Fig. 1b).

Role of GALNT2 on mature adipocyte proportion and lipid accumulation

Adipogenesis was then induced for 15 days in T_0 GFP and T_0 GALNT2 cells. Figure 2a shows representative micrographs of undifferentiated T_0 cells (images 1 and 4) and

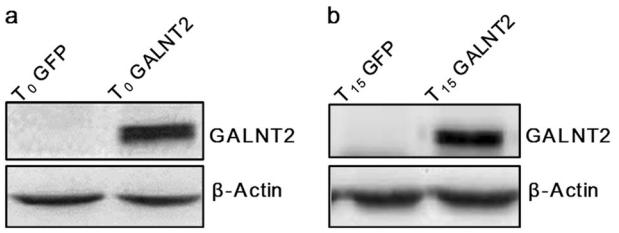

Fig. 1 Over-expression of GALNT2 in 3T3-L1 cells. 3T3-L1 cells were transduced with either pLX304_GALNT2 or pLV-CMV-GFP as described in Materials and Methods. GALNT2 expression was evaluated at T_0 (**a**) and T_{15} (**b**) by western blot. In brief, equal amounts of protein from cell lysates were separated by SDS-PAGE and probed with GALNT2 (upper blot) or β-actin (lower blot) specific antibodies

mature adipocytes, either $T_{15}R-$ (images 2 and 5) or $T_{15}R+$(images 3 and 6). In GFP cells, the apparent proportion of mature adipocytes progressively increased from T_0 to $T_{15}R-$ and to $T_{15}R+$ (images 1–3). A similar, though stronger, increase was observed in GALNT2 cells (images 4–6). In fact, as compared to GFP cells, the proportion of mature adipocytes appeared to be higher in their GALNT2 counterparts (image 5 vs. 2 and image 6 vs. 3). In addition, the proportion of mature adipocytes in $T_{15}R-$GALNT2 cells looked quite similar to that in $T_{15}R+$GFP cells (image 5 vs. 3), as if the magnitude of GALNT2 effect were similar to that of rosiglitazone.

Figure 2b (left side) shows that, as compared to T_0 GFP cells, lipid content was significantly increased in $T_{15}R-$ (1.7 fold-increase) and even more in $T_{15}R+$ (2.2 fold-increase) GFP cells. A similar, though stronger, trend was observed also in GALNT2 cells (Fig. 2b, right side), with differences vs. their T_{15} GFP counterparts becoming significant ($p = 0.01$) for the $T_{15}R+$condition (Fig. 2b, black bars). It is worth noticing that lipid accumulation in $T_{15}R-$GALNT2 cells was virtually identical to that in $T_{15}R+$GFP cells (Fig. 2b, right side white bar vs. left side black bar).

Very similar results were obtained when intracellular triglycerides levels were measured. In fact, as compared to T_0 GFP cells (Fig. 2c, left side), triglycerides were significantly increased in $T_{15}R-$ (3.5-fold-increase) and even more in $T_{15}R+$ (4.2-fold-increase) GFP cells. An even stronger trend was observed in GALNT2 cells (Fig. 2c, right side), with differences vs. their T_{15} GFP counterparts being significant for both $T_{15}R-$ ($p = 0.019$) and $T_{15}R+$ ($p = 0.034$) conditions (Fig. 2c, white bars and black bars, respectively). Also in this case, it is worth noticing that triglycerides accumulation in $T_{15}R-$GALNT2 cells was virtually identical to that in $T_{15}R+$GFP cells (Fig. 2c, right side white bar vs. left side black bar). Then, for both lipid accumulation and triglycerides content, these results parallel those referring to the proportion of mature adipocytes and give further support to the concept that the magnitude of GALNT2 stimulatory effect on adipogenesis is similar to that of rosiglitazone.

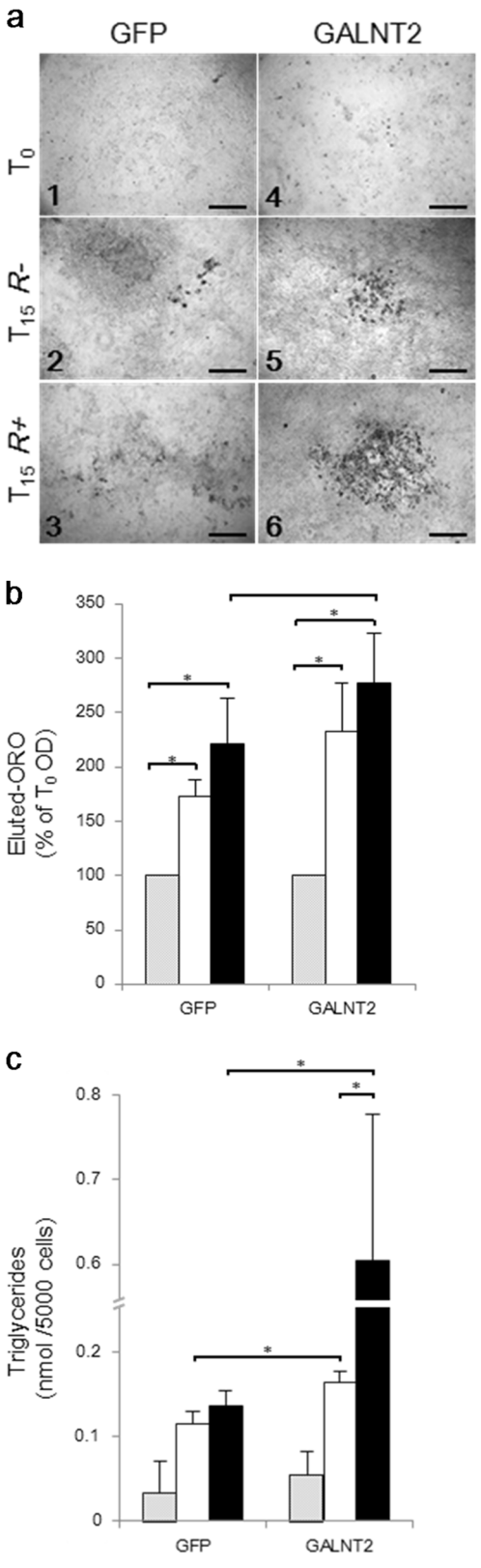

◀ **Fig. 2** Role of GALNT2 on adipocyte proportion and lipid accumulation. GFP and GALNT2 cells were differentiated into adipocytes either with (*R*+) or without (*R*−) rosiglitazone. **a** shows Oil-red-O (ORO) staining (see Material and Methods) of lipids in representative 5 × (gray-scale) microscopy images of cells at T_0 and T_{15}. Scale bar = 500 µm. **b** shows quantitative analysis of eluted ORO (see Material and Methods) at T_0 and T_{15}. Bars represent eluted-ORO optical density (OD) from both $T_{15}R-$ and $T_{15}R+$ (white and black bars, respectively) cells, expressed as percentage of that from T_0 (gray bars) cells. **c** shows quantitative analyses of extracted triglycerides (see Material and Methods) at T_0 and T_{15}. Bars represent intracellular triglycerides from T_0 (gray bars) and both $T_{15}R-$ and $T_{15}R+$ (white and black bars, respectively) expressed as nmol/5000 cells. Data are means ± SE of 6 independent experiments. *2 sided $p < 0.05$ by Student's *t*-test

Role of GALNT2 on droplet morphology in mature adipocytes

Representative LD images in mature adipocytes are shown in Fig. 3a. In both cell lines, rosiglitazone treatment increased LD size and roundness (Fig. 3a, panel 2 vs. 1 and panel 4 vs. 3). Notably, LD size in $T_{15}R-$GALNT2 cells looked similar if not larger than that in $T_{15}R+$GFP cells (Fig. 3a, panel 3 vs. 2), again pointing to an effect of GALNT2 over-expression of a similar magnitude of rosiglitazone.

LD morphology was measured by means of 2 shape descriptors (Figs. 3b, c), including area and size. As compared to their $T_{15}R-$ counterparts, LD area was significantly increased in both $T_{15}R+$GFP and GALNT2 cells (Fig. 3b), while LD size was significantly higher only in $T_{15}R+$GFP cells, with only mild, non-significant increase showed by GALNT2 cells (Fig. 3c). LD area and size in GALNT2 cells were significantly increased as compared to their GFP counterparts, both without and with rosiglitazone treatment (Figs. 3b, c). Notably, LD area and size in $T_{15}R$-GALNT2 cells were significantly greater than those of $T_{15}R+$GFP cells (Figs. 3b, c), thus indicating that the effect of GALNT2 over-expression in modulating also this additional adipogenesis-related phenotype is at least similar if not larger than that of rosiglitazone.

Taken altogether, our data indicate that GALNT2 has a positive role on 3T3-L1 differentiation, lipid accumulation and LD morphology whose magnitude resembles very much that of rosiglitazone.

Role of GALNT2 on insulin signaling

Given that adipocyte maturation is under the control of insulin signaling, time course experiments of insulin-induced IR, IRS1, AKT and JNK1/JNK2 phosphorylation were carried out, so to get deeper insights on the molecular mechanisms underlying GALNT2 effect on adipocyte enlargement. In both GFP and GALNT2 cells, a clear insulin stimulation of IR β-subunit auto-phosphorylation, $IRS1^{Tyr895}$ and AKT^{Ser473} phosphorylation (Figs. 4a–c, respectively) was observed at T_0, T_9 and T_{15}. In GALNT2 preadipocytes, insulin-induced IR was significantly higher than that observed in GFP cells (Fig. 4a, T_0). This GALNT2 stimulatory effect was no longer observed during adipocyte maturation (Fig. 4a, T_9), and totally reversed at late stage maturation, where GALNT2 enlarged adipocytes showed a significantly reduced insulin-induced IR phosphorylation (Fig. 4a, T_{15}). A virtually identical trend of GALNT2 effect was observed for both insulin-induced IRS1 and AKT activation (Figs. 4b, c), though statistical significance for IRS1 stimulation in preadipocytes (T_0) was not reached.

Finally, as compared to their GFP counterparts, insulin-induced $JNK1/JNK2^{Thr183/Tyr185}$ was similar in GALNT2

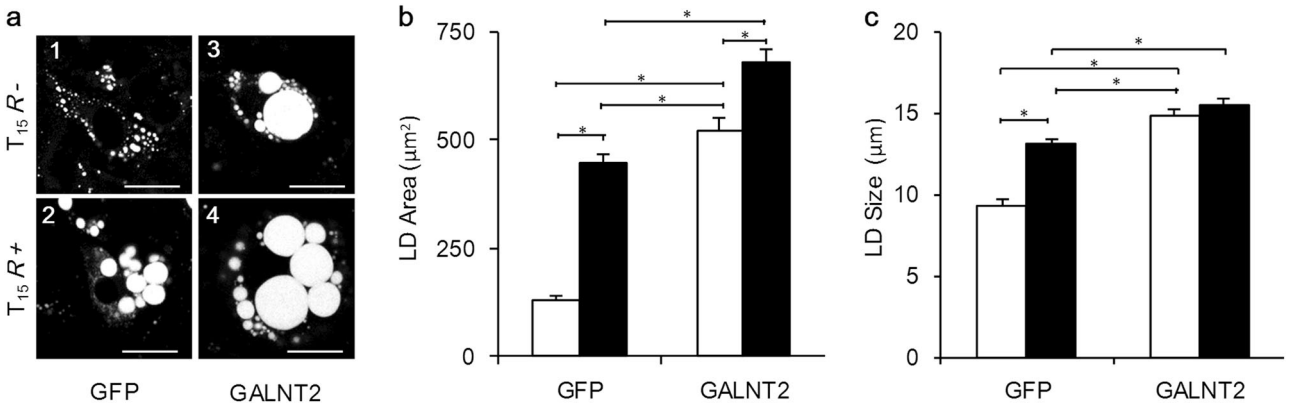

Fig. 3 Effect of GALNT2 on lipid droplet morphology in mature adipocytes. GFP and GALNT2 cells were differentiated into adipocytes with (*R*+) or without (*R*−) rosiglitazone and stained with Adipo Red as described in Material and Methods. Panel **a** shows representative details of Adipo Red-stained LD from ×40 confocal microscopy images of $T_{15}R-$ and $T_{15}R+$cells. Scale bar = 25 µm. **b**, **c** show quantitative analyses of LD area and size, respectively. Bars represent micron-scale measurements of LD area (**b**) and size (**c**) from both $T_{15}R-$ and $T_{15}R+$ (white and black bars, respectively) cells. Data are means ± SE of LD measurements from at least 30 fields of view from 2 independent experiments. *2 sided $p < 1 \times 10^{-5}$ by Student's *t*-test

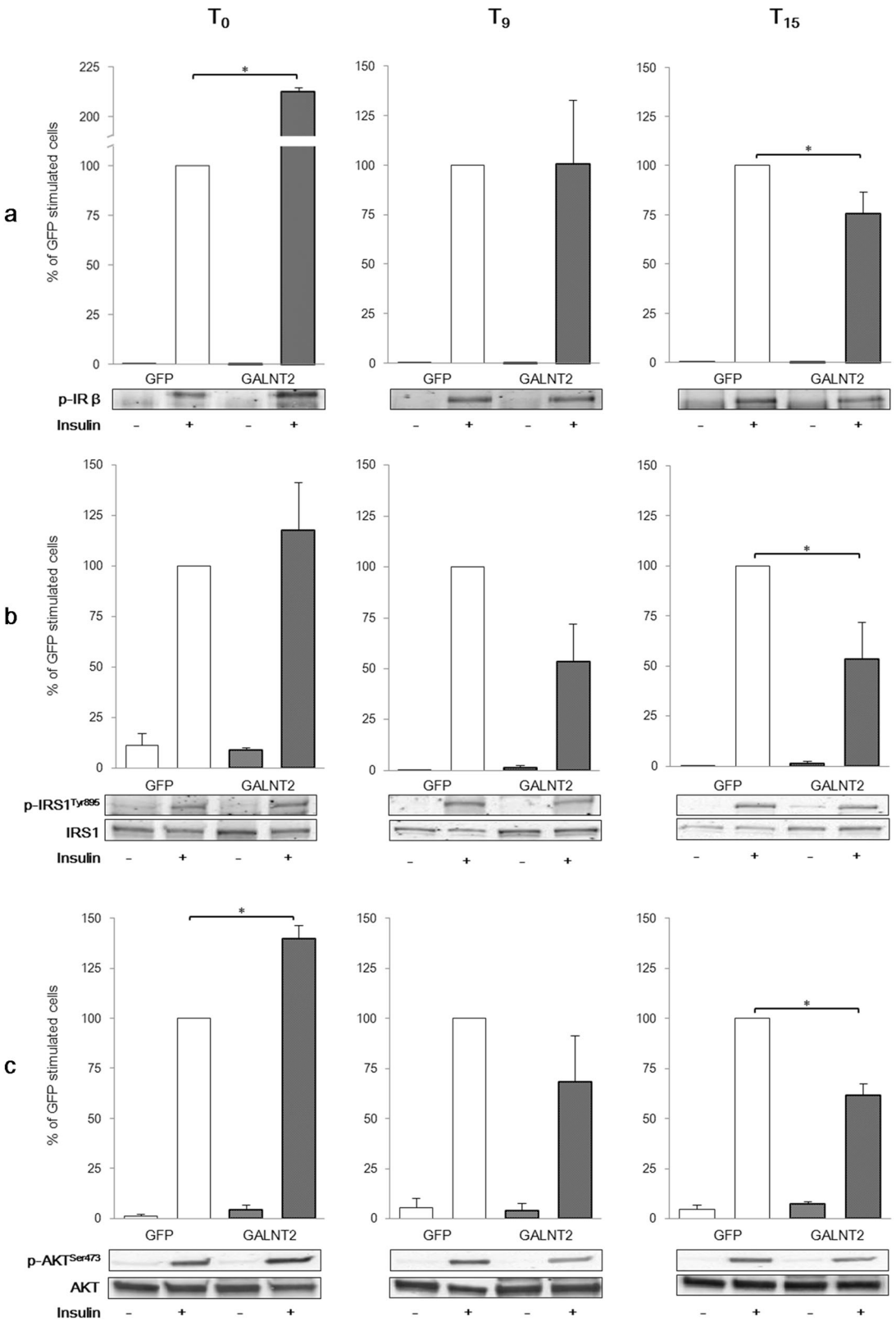

cells at T_0 (109% ± 9 SE of GFP stimulated cells, $n = 3$), T_9 (99% ± 11 SE of GFP stimulated cells, $n = 3$) and T_{15} (94% ± 8.3 SE of GFP stimulated cells, $n = 3$). Representative experiments at each time point are shown in Supplementary Information 2. These data suggest that GALNT2 effect on adipogenesis is not modulated by JNK signaling.

◀ **Fig. 4** Role of GALNT2 on insulin signaling. GFP and GALNT2 cells were stimulated with 10^{-7} M insulin and then IR β-subunit (**a**), $IRS1^{Tyr895}$ (**b**) and AKT^{Ser473} (**c**) phosphorylation were evaluated by Western blot analyses as described in Materials and Methods. **a** Bars represent quantitative analysis of IR β-subunit phosphorylation expressed as percentage of that observed in insulin-stimulated GFP cells (white bars) at T_0 ($n = 3$), T_9 ($n = 3$), and T_{15} ($n = 6$). **b** Bars represent quantitative analyses of insulin-induced $IRS1^{Tyr895}$ phosphorylation/IRS1 OD ratio expressed as percentage of that observed in insulin-stimulated GFP cells (white bars) at each time points (T_0, T_9 and T_{15}, $n = 3$ at all time points). **c** Bars represent quantitative analyses of insulin-induced AKT^{Ser473} phosphorylation/AKT OD ratio, expressed as percentage of that observed in insulin-stimulated GFP cells (white bars) at T_0 ($n = 3$), T_9 ($n = 3$) and T_{15} ($n = 6$). All data are means ± SE. *2 sided $p < 0.05$ by Student's *t*-test. A representative blot for each experimental condition is shown

In all, data in preadipocytes are definitively consistent with the reported positive role of GALNT2 on insulin sensitivity in other cell types [12], which in turn stimulates adipocyte maturation and eventually adipocyte enlargement [17]. Conversely, the reduced insulin signaling in mature GALNT2 adipocytes is fully compatible with the well-known decreased insulin sensitivity characterizing enlarged adipocytes [18, 19].

Role of GALNT2 on the expression of ENPP1 and genes related to adipogenesis

Firstly, the expression of *Enpp1*, a negative modulator of insulin signaling whose expression in liver cells is decreased by GALNT2 [12], was evaluated. In fact, as compared to GFP counterparts, in GALNT2 cells *Enpp1* expression was similar at T_0 (1.15 fold, $n = 3$) and was progressively down-regulated at T_9 (1.6 fold-decrease, n = 3) and even more strikingly at T_{15} (6.9-fold-decrease, $n = 3$). Of note, such *Enpp1* down-regulation was not paralleled by changes in *Galnt2* expression in T_9 and T_{15} as compared to T_0 (fold-change at both time points ranging from −1.4 to 1.2, $n = 3$). Finally, also no changes were observed during adipogenesis in the expression of *hGALNT2* in transfected cells (data not shown, $n = 3$).

Then, expression levels of 72 adipogenesis-related genes were measured during adipocyte maturation, at T_0 (Fig. 5a), T_9 (Fig. 5b) and T_{15} (Fig. 5c). At each time point, several genes were at least 2-fold changed in GALNT2 cells as compared to their GFP counterparts. In details, 6 genes were either increased (*Hes1*) or decreased (*Agt, Foxc2, Klf15, Ucp1, Wnt5a*) at T_0, 13 were either increased (*Adig, Adipoq, Retn, Bmp4, Hes1*) or decreased (*Agt, Cebpb, Gata2, Lipe, Rxra, Tsc22d3, Ucp1, Wnt5a*) at T_9, and 21 were either increased (*Adig, Adipoq, Adrb2, Cebpa, Fabp4, Nr1h3, Retn, Wnt5b*) or decreased (*Agt, Egr2, Fgf2, Gata2, Insr, Lipe, Runx1t1, Rxra, Slc2a4, Tsc22d3, Ucp1, Wnt1, Wnt5a*) at T_{15}. Of these 21 genes, 3 were already downregulated at T_0 and maintained as such also at T_9 (*Agt, Ucp1, Wnt5a*), while 7 were either upregulated (*Adig, Adipoq, Retn*) or downregulated (*Gata2, Lipe, Rxra, Tsc22d3*) only starting from T_9.

In all, these results strongly suggest that GALNT2 induces a coordinated and time-dependent change in the expression of adipocyte maturation key genes which is likely to have played a role on the different adipogenesis observed in GALNT2 as compared to GFP cells.

Discussion

Our previous work pointed GALNT2 as a positive modulator of insulin signaling in human liver cells [12, 18–21]. Based on the notion that *GALNT2* expression is increased in subcutaneous adipose tissue of obese individuals [13] and that insulin signaling stimulates adipocytes differentiation [3], we have now tested the hypothesis that GALNT2 exerts a stimulatory role on adipogenesis.

As a matter of fact, our data clearly show that in 3T3-L1 mouse cells GALNT2 stimulates adipogenesis as indicated by increased proportion of mature adipocytes, intracellular lipids, including triglycerides, and lipid droplets dimension.

Of note, the magnitude of GALNT2 stimulatory effect on adipogenesis was relevant, being superimposable to that exerted by rosiglitazone [5], a potent stimulator of adipogenesis [22] known to cause weight gain in patients with type 2 diabetes [5].

GALNT2 stimulatory effect on adipogenesis was paralleled by improved insulin signaling in preadipocytes. This effect was abolished during adipocyte maturation and completely reversed at late stage maturation as a possible consequence of adipocytes enlargement [18–21]. These data suggest that if adipocytes are pushed to maturation from the very early stages, the whole adipogenesis until late stage and ultimate adipocytes enlargement is heavily compromised.

During adipogenesis GALNT2 cells were also characterized by *Enpp1* down-regulation, a negative modulator of insulin signaling [23–25], thus confirming previous data we reported in human cultured liver cells over-expressing *GALNT2* [12]. Taken together these two piece of data strongly suggest that during cell differentiation GALNT2 down-regulated *Enpp1*, so increasing insulin signaling and stimulating adipogenesis [12, 26]; however, once adipogenesis was established, the positive GALNT2 effect on insulin signaling, was eventually overwhelmed by the opposite deleterious effect on the same insulin signaling ineludibly exerted by adipocytes enlarging [18–21]. This latter phenomenon, which is likely part of the adipocyte homeostatic response aimed at impeding further enlargement under conditions of continuous insulin stimulation

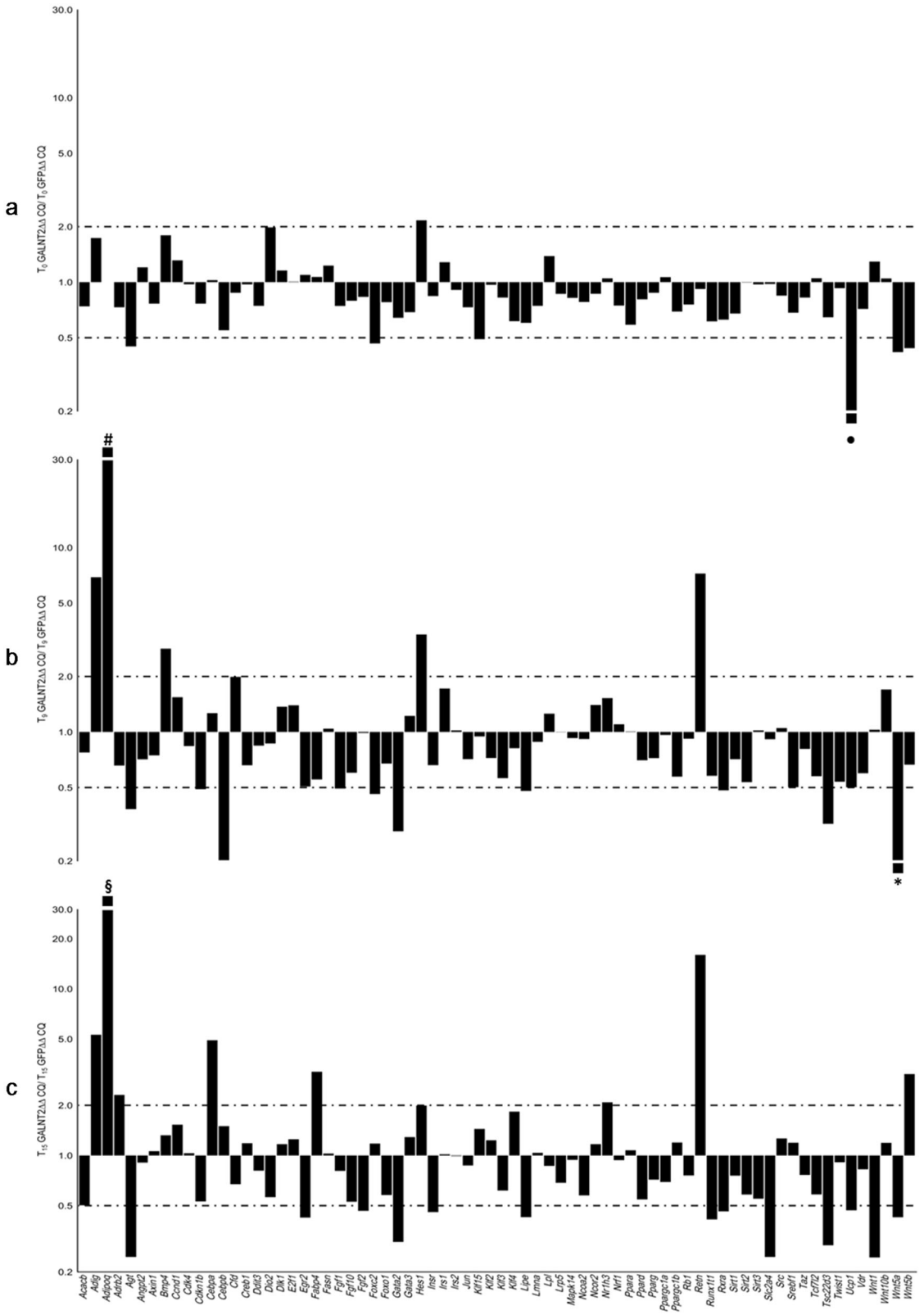

[27–29], is paralleled and may be, therefore, at least partly explained by the strikingly increased levels of resistin gene (*Retn*) [30] observed during adipogenesis in GALNT2 over-expressing cells.

◀ **Fig. 5** Role of GALNT2 on adipogenesis-related gene expression. Expression levels of 72 adipogenesis-related genes were measured by real time PCR and calculated as ΔΔCQ values as described in Materials and Methods. Bars are gene expression fold-changes in GALNT2 vs. GFP cells at T_0, T_9 and T_{15} (**a**–**c**, respectively). Data are from 3 independent experiments. Dotted lines indicate either increased or decreased 2-fold change. *Adipoq* expression was undetectable in T_0 cells. Symbols indicate real fold-changes in GALNT2 vs. GFP cells as it follows: • = 0.04; # = 70.7; * = 0.07; § = 115

The insulin resistant phenotype we observed in GALNT2 mature adipocytes might be also explained by ceramides-dependent mechanisms, known to inhibit insulin signaling, through the PKR/JNK pathway [31]. However, although we do acknowledge that lack of ceramides data is a limitation of our study, data showing no changes between GFP and GALNT2 cells in insulin-induced JNK phosphorylation, make unlikely that ceramides-dependent mechanisms are involved in reducing insulin signaling in GALNT2 mature adipocytes.

In addition, it cannot be excluded that GALNT2 affects adipogenesis also independently of insulin signaling. For example, the coordinated change in the expression of key maturation genes we observed along the whole course of adipogenesis may have also played a role in mediating GALNT2 promoted adipocyte enlargement. In fact, the expression of some genes that are either up-regulated (*Adig, Retn, Nr1h3*) or down-regulated (*Ucp1, Slc2a4, Lipe, Fgf2, Tcs22d3*) in GALNT2 cells, has been previously reported to associate with adipocytes lipid storage [32] and adiposity measures [33–39], toward a coherent direction with our present findings.

GALNT2 is involved in O-glycosylation (i.e., the sequential addition of different monosaccharides to proteins) an intracellular processing step of utmost importance [40]. This also may have played a role in mediating GALNT2 effect on adipogenesis. At this regard, increased GALNT2 downstream glycosylation processes up-regulate *CEBPa* and *AdipoQ* [41], whose expression was in fact increased during adipocytes maturation in GALNT2 cells.

Finally, no matter the mechanisms mediating its effects on adipogenesis, our finding envisions GALNT2 as an attractive drug-target for tackling increased expansion of adipose tissue and, therefore, the worldwide epidemic of obesity and related dramatic sequelae. In fact, both gene silencing and binding prevention tools are novel strategies hoped to pave the way for inventing new treatments in the field of metabolic diseases [42, 43]. Conversely, since thiazolinediones have been proposed for treating lipodystrophies of any origin [5, 44, 45], and since our data show that the magnitude of GALNT2 stimulatory effect on adipogenesis is similar to that of rosiglitazone, one could also speculate that GALNT2 up-regulation might be a rational approach for treating these conditions.

In conclusion, our data indicate that GALNT2 is a positive modulator of adipocytes insulin signaling and point it as a novel promoter of adipogenesis which eventually causes adipocytes enlargement. Further studies are needed to get deeper insights on the precise mechanisms by which GALNT2 exerts its effects on adipocyte biology and to address whether it may become a new target for treating states of abnormal expansion of adipose tissue.

Acknowledgements This work was supported by the Italian Ministry of Health Ricerca Corrente 2017-2019 (A.M., R.D.P., V.T.).

Compliance with ethical standards

Conflict of interest The authors declare that they have no conflict of interest.

References

1. WHO. Noncommunicable Diseases, Progress Monitor 2017. WHO, 72nd session of the UN General Assembly; 2017.
2. Reaven GM. Role of insulin resistance in human disease. Diabetes. 1988;37:1595–607.
3. Czech MP, Tencerova M, Pedersen DJ, Aouadi M. Insulin signalling mechanisms for triacylglycerol storage. Diabetologia. 2013;56:949–64.
4. Swinburn BA, Nyomba BL, Saad MF, Zurlo F, Raz I, Knowler WC, et al. Insulin resistance associated with lower rates of weight gain in Pima Indians. J Clin Invest. 1991;88:168–73.
5. Yki-Jarvinen H. Thiazolidinediones. N Engl J Med. 2004;351:1106–18.
6. White T, Bennett EP, Takio K, Sorensen T, Bonding N, Clausen H. Purification and cDNA cloning of a human UDP-N-acetyl-alpha-D-galactosamine:polypeptide N-acetylgalactosaminyltransferase. J Biol Chem. 1995;270:24156–65.
7. Schjoldager KT, Joshi HJ, Kong Y, Goth CK, King SL, Wandall HH, et al. Deconstruction of O-glycosylation—GalNAc-T isoforms direct distinct subsets of the O-glycoproteome. EMBO Rep. 2015;16:1713–22.
8. Kathiresan S, Willer CJ, Peloso GM, Demissie S, Musunuru K, Schadt EE, et al. Common variants at 30 loci contribute to polygenic dyslipidemia. Nat Genet. 2009;41:56–65.
9. Teslovich TM, Musunuru K, Smith AV, Edmondson AC, Stylianou IM, Koseki M, et al. Biological, clinical and population relevance of 95 loci for blood lipids. Nature. 2010;466:707–13.
10. Khetarpal SA, Schjoldager KT, Christoffersen C, Raghavan A, Edmondson AC, Reutter HM, et al. Loss of function of GALNT2 lowers high-density lipoproteins in humans, nonhuman primates, and rodents. Cell Metab. 2016;24:234–45.
11. Di Paola R, Marucci A, Trischitta V. GALNT2 effect on HDL-cholesterol and triglycerides levels in humans: evidence of pleiotropy? Nutr Metab Cardiovasc Dis. 2017;27:281–2.
12. Marucci A, Cozzolino F, Dimatteo C, Monti M, Pucci P, Trischitta V, et al. Role of GALNT2 in the modulation of ENPP1 expression, and insulin signaling and action. Biochimica et Biophysica Acta Mol Cell Res. 2013;1833:1388–95.
13. Lee YH, Nair S, Rousseau E, Allison DB, Page GP, Tataranni PA, et al. Microarray profiling of isolated abdominal subcutaneous adipocytes from obese vs non-obese Pima Indians: increased

expression of inflammation-related genes. Diabetologia. 2005;48:1776–83.
14. Carlotti F, Bazuine M, Kekarainen T, Seppen J, Pognonec P, Maassen JA, et al. Lentiviral vectors efficiently transduce quiescent mature 3T3-L1 adipocytes. Mol Ther. 2004;9:209–17.
15. Graham FL, van der Eb AJ. A new technique for the assay of infectivity of human adenovirus 5 DNA. Virology. 1973;52:456–67.
16. Vandesompele J, De Preter K, Pattyn I, Poppe B, Van Roy N, De Paepe A, et al. Accurate normalization of real-time quantitative RT-PCR data by geometric averaging of multiple internal control genes. Genome Biol. 2002;3:34–1.
17. Rosen ED, MacDougald OA. Adipocyte differentiation from the inside out. Nat Rev Mol Cell Biol. 2006;7:885–96.
18. Czech MP. Cellular basis of insulin insensitivity in large rat adipocytes. J Clin Invest. 1976;57:1523–32.
19. Arner E, Westermark PO, Spalding KL, Britton T, Ryden M, Frisen J, et al. Adipocyte turnover: relevance to human adipose tissue morphology. Diabetes. 2010;59:105–9.
20. Guilherme A, Virbasius JV, Puri V, Czech MP. Adipocyte dysfunctions linking obesity to insulin resistance and type 2 diabetes. Nat Rev Mol Cell Biol. 2008;9:367–77.
21. Olefsky JM. Mechanisms of decreased insulin responsiveness of large adipocytes. Endocrinology. 1977;100:1169–77.
22. Shao D, Lazar MA. Peroxisome proliferator activated receptor gamma, CCAAT/enhancer-binding protein alpha, and cell cycle status regulate the commitment to adipocyte differentiation. J Biol Chem. 1997;272:21473–8.
23. Maddux BA, Sbraccia P, Kumakura S, Sasson S, Youngren J, Fisher A, et al. Membrane glycoprotein PC-1 and insulin resistance in non-insulin-dependent diabetes mellitus. Nature. 1995;373:448–51.
24. Abate N, Chandalia M, Di Paola R, Foster DW, Grundy SM, Trischitta V. Mechanisms of disease: Ectonucleotide pyrophosphatase phosphodiesterase 1 as a "gatekeeper" of insulin receptors. Nat Clin Pract Endocrinol Metab. 2006;2:694–701.
25. Di Paola R, Caporarello N, Marucci A, Dimatteo C, Iadicicco C, Del Guerra S, et al. ENPP1 affects insulin action and secretion: evidences from in vitro studies. PLoS ONE. 2011;6:e19462.
26. Marucci A, Miscio G, Padovano L, Boonyasrisawat W, Doria A, Trischitta V, et al. A functional variant in the gene 3' untranslated region regulates HSP70 expression and is a potential candidate for insulin resistance-related abnormalities. J Intern Med Suppl. 2010;267:237–40.
27. Kern PA, Saghizadeh M, Ong JM, Bosch RJ, Deem R, Simsolo RB. The expression of tumor necrosis factor in human adipose tissue. Regulation by obesity, weight loss, and relationship to lipoprotein lipase. J Clin Invest. 1995;95:2111–9.
28. Uysal KT, Wiesbrock SM, Marino MW, Hotamisligil GS. Protection from obesity-induced insulin resistance in mice lacking TNF-alpha function. Nature. 1997;389:610–4.
29. Pal A, Barber TM, Van de Bunt M, Rudge SA, Zhang Q, Lachlan KL, et al. PTEN mutations as a cause of constitutive insulin sensitivity and obesity. N Engl J Med. 2012;367:1002–11.
30. Schwartz DR, Lazar MA. Human resistin: found in translation from mouse to man. Trends Endocrinol Metab. 2011;22:259–65.
31. Hage Hassan R, Pacheco de Sousa AC, Mahfouz R, Hainault I, Blachnio-Zabielska A, Bourron O, et al. Sustained action of ceramide on the insulin signaling pathway in muscle cells: implication of the double-stranded Rna-activated protein kinase. J Biol Chem. 2016;291:3019–29.
32. Hong Y-H, Hishikawa D, Miyahara H, Tsuzuki H, Nishimura Y, Gotoh C, et al. Up-regulation of adipogenin, an adipocyte plasma transmembrane protein, during adipogenesis. Mol Cell Biochem. 2005;276:133–41.
33. Dahlman I, Nilsson M, Jiao H, Hoffstedt J, Lindgren CM, Humphreys K, et al. Liver X receptor gene polymorphisms and adipose tissue expression levels in obesity. Pharmacogenet Genom. 2006;16:881–9.
34. Kim S, Ahn C, Bong N, Choe S, Lee DK. Biphasic effects of FGF2 on adipogenesis. PLoS ONE. 2015;10:1–12.
35. Poletto AC, David-Silva A, Yamamoto APDM, Machado UF, Furuya DT. Reduced Slc2a4/GLUT4 expression in subcutaneous adipose tissue of monosodium glutamate obese mice is recovered after atorvastatin treatment. Diabetol Metab Syndr. 2015;7:1–6.
36. Lee MJ, Yang RZ, Karastergiou K, Smith SR, Chang JR, Gong DW, et al. Low expression of the GILZ may contribute to adipose inflammation and altered adipokine production in human obesity. J Lipid Res. 2016;57:1256–63.
37. Bazhan NM, Baklanov AV, Piskunova JV, Kazantseva AJ, Makarova EN. Expression of genes involved in carbohydrate-lipid metabolism in muscle and fat tissues in the initial stage of adult-age obesity in fed and fasted mice. Physiol Rep. 2017;5:1–10.
38. Jonas MI, Kurylowicz A, Bartoszewicz Z, Lisik W, Jonas M, Domienik-Karlowicz J, et al. Adiponectin/resistin interplay in serum and in adipose tissue of obese and normal-weight individuals. Diabetol Metab Syndr. 2017;9:1–9.
39. Nascimento EBM, Sparks LM, Divoux A, van Gisbergen MW, Broeders EPM, Jörgensen JA, et al. Genetic markers of brown adipose tissue identity and in vitro brown adipose tissue activity in humans. Obesity. 2017;26:135–40.
40. Bennett EP, Mandel U, Clausen H, Gerken TA, Fritz TA, Tabak LA. Control of mucin-type O-glycosylation: a classification of the polypeptide GalNAc-transferase gene family. Glycobiology. 2012;22:736–56.
41. Wollaston-Hayden EE, Harris RBS, Liu B, Bridger R, Xu Y, Wells L. Global O-GlcNAc levels modulate transcription of the adipocyte secretome during chronic insulin resistance. Front Endocrinol. 2015;5:223.
42. Czech MP, Aouadi M, Tesz GJ. RNAi-based therapeutic strategies for metabolic disease. Nat Rev Endocrinol. 2011;7:473–84.
43. Fountas A, Diamantopoulos LN, Tsatsoulis A. Tyrosine kinase inhibitors and diabetes: a novel treatment paradigm? Trends Endocrinol Metab. 2015;26:643–56.
44. Ishihara K, Takahashi I, Tsuchiya Y, Hasegawa M, Kamemura K. Characteristic increase in nucleocytoplasmic protein glycosylation by O-GlcNAc in 3T3-L1 adipocyte differentiation. Biochem Biophys Res Commun. 2010;398:489–94.
45. Agostini M, Schoenmakers E, Beig J, Fairall L, Szatmari I, Rajanayagam O, et al. A pharmacogenetic approach to the treatment of patients with PPARG mutations. Diabetes. 2018;67:1086–92.